Carbohydrate Polymers 98 (2013) 568–573

Contents lists available at SciVerse ScienceDirect

Carbohydrate Polymers

journal homepage: www.elsevier.com/locate/carbpol

Formation of nanometal particles in the dialdehyde starch matrix

Karen Khachatryan*, Gohar Khachatryan, Maciej Fiedorowicz, Andrzej Para, Piotr Tomasik

Department of Chemistry and Physics, Agricultural University, Balicka Street 122, 30 149 Krakow, Poland

ARTICLE INFO

Article history:
Received 20 March 2013
Received in revised form 9 May 2013
Accepted 18 June 2013
Available online 26 June 2013

Keywords:
Biocomposites
Nanogold
Nanometals
Nanosilver

ABSTRACT

Environmentally friendly method of the preparation of dialdehyde starch (DAS) based composites containing nanosilver (DAS/Ag) and nanogold (DAS/Au) as reducing and protecting agents was developed. UV–vis spectroscopy, transmission electron microscopy (TEM) and X-ray diffraction (XRD) confirmed formation of about 10 nm ball shaped Ag and Au nanoparticles situated within the polysaccharide template. Thermal properties of the composites were characterized involving differential scanning calorimetry (DSC), whereas molecular weights of polysaccharide chains of the matrix were estimated with the size exclusion chromatography coupled with multiangle laser light scattering and refractometric detectors (HPSEC-MALLS-RI).

Formation of nanosilver and nanogold containing composites led to induction of the polymerization and/or crosslinking reactions of DAS molecules, resulting in a significant rise of molecular weight of polysaccharide chains constituting DAS/Ag and DAS/Au composite templates.

1. Introduction

Nanotechnology could be regarded as a new branch of material engineering science allowing fabrication of materials with unique properties. Among others nanomaterials, polymer-metal nanoparticle composites received much attention in recent years for their application in optoelectronics, nonlinear optical devices and color filters (Datta, Srinivasan, Balaram, & Eswaramoorthy, 2008).

Recently several methods of synthesis of nanometal powders were reported (Bradley, 1994; Brown & Smith, 1980; Datta et al., 2008; Frens, 1973; Hayat, 1989; Hyatt & Eaton, 1993; Schmid, 1992; Turkevitch, Stevenson, & Hillier, 1951). Methods of the nanometal syntheses mostly rely on a reduction of metal salts in the presence of a stabilizer. Gold, silver, and copper salts used to be reduced with sodium borohydride (Brust, Walker, Bethell, Schiffrin, & Whyman, 1994; Fu, Yang, Li, Yu, & Long, 2006; Hiramatsu & Osterloh, 2004; Leff, Brandt, & Heath, 1996), citiric acid and its salts (Hyatt & Eaton, 1993; Turkevitch et al., 1951; Yonezawa & Kunitake, 1999), NaH_2PO_2 (Zhua, Zhang, & Yin, 2004), hydrazine (Adhyapak, Singh, Vijayan, Aiyer, & Khanna, 2007; Pal, Shah, & Devi, 2007; Wu & Chen, 2004) and alcohols (Kim, 2007). To prevent a common aggregation of nanocrystals formed, surfactants and/or broad variety of synthetic polymers are used. Surfactants, most commonly cetyl tetramethylammonium bromide (CTAB) (Fu et al., 2006; Wu & Chen, 2004), thiols (Brust et al., 1994; Giersig & Mulvaney, 1993), xanthans (Tzhayik, Sawant, Efrima, Kovalev, & Klug, 2002) and citric acid salts (Huang, Guo, Weng, & Gu, 2006), by coating surface of nanoparticles, not only inhibit their agglomeration but also introduce the nanocrystals into solvents (Daniel & Astruc, 2004; Shon & Choo, 2003; Templeton, Wuelfing, & Murray, 2000). However, chemical binding of surfactant molecules to the nanometal surface, could hamper some properties of nanostructures. Therefore, synthesis of nanometals in the polymer matrix, as an alternative method of preventing aggregation, is frequently in use. Polymers, as a matrix for nanometals roughly spread into two groups: (i) synthetic non-biodegradable polymers such as poly(vinyl alcohol) (PVA) (Kang & Wu, 2006; Zhua et al., 2004), poly(vinylpyrrolidone) (PVP) and other N-containing polymers like nylon, polyurethanes (Pobedinsky & Johnston, 2010; Wu & Chen, 2004; Zhang, Fu, Fan, & Zhou, 2005), polyimides (Park, Lee, Kim, & Oh, 2009), sulfonated poly(ether ether ketone) (Li, Hao, & Hui, 2007), polyesters (Lin, Tseng, & Chien, 2006), organosilicon polymers (Saulon et al., 2008), poly(acrylamide)/ethylene vinyl acetate (Xu, Feng, & Cao, 2008) and (ii) biodegradable polymers either directly isolated from plants (i.e. polysaccharides, proteins, polypeptides, polynucleotides), their modificates such as β-chitin (Kumar et al., 2010) and hydroxypropylmethyl cellulose(Dabbagh, Moghimipour, Ameri, & Sayfoddin, 2008), and polymers produced by classical chemical synthesis using renewable bio-based monomers or mixed sources of biomass and petroleum (i.e. polylactic acid, other poly(hydroxyl- and thiolo-fatty acids) and their polyesters (Tokuda, Obata, & Kasuga, 2009; Vasilev, Gulliver, Khinast, & Riman, 2009).

* Corresponding author. Tel.: +48 12 6624139; fax: +48 12 6624336.
E-mail addresses: rrchacza@cyf-kr.edu.pl, karen@khachatryan.com (K. Khachatryan).

0144-8617/$ – see front matter © 2013 Elsevier Ltd. All rights reserved.
http://dx.doi.org/10.1016/j.carbpol.2013.06.032

Recently growing interest in use of biodegradable polymers as a matrix for formation of nanostructures falls in line with development of environmentally benign methods of the nanometals synthesis. Such approach called "green chemistry" provides stable nanometal structures embedded in polymers matrix eliminating the use of harmful solvents and reducing agents. Moreover, such materials facilitate an integration of nanometals with biologically relevant systems. For example, in such environmentally benign way formation of Au and Ag nanoparticles in polysaccharide gels, which served both as reducing agents and stabilizers, was reported (Huang & Yang, 2004). Raveendran, Fu, & Wallen (2003) described formation of nanosilver and nanogolds structures of the size below 10 nm involving reduction with glucose and water soluble starch as stabilizer.

In this paper, we report an environmentally benign, green, method for the preparation of Au and Ag nanoparticles in dialdehyde starch matrix, using dialdehyde starch as the both reducing and protecting agent. Dialdehyde starch (DAS) of 9% degree of oxidation (DE) was prepared from potato starch according to Para, Karolczyk-Kostuch, Hajdon, & Tomasik (2000), that is, using periodate with electrochemical recovery of the oxidant. Prepared materials are supposed to combine well known bactericidal properties of nano Ag (Pal, Shah, et al., 2007; Pal, Tak, et al., 2007) and nanoAu (Merchant, 1998) with antiviral properties of DAS (Song, Cruz, Farrah, & Baney, 2009).

DAS/Ag and DAS/Au nanocomposites were characterized with UV–vis and IR spectrometries, X-ray diffraction patterns, transmission electron microscopy (TEM) and scanning electron microscopy (SEM). The absolute molecular weights, radii of gyration, R_g, and thermodynamic properties of obtained composites are also given.

2. Experimental

2.1. Synthesis of metal nanoparticles-DAS composite

DAS/nanoAg and DAS/nanoAu composites were prepared from DAS (DE 9%) (Fiedorowicz & Para, 2006; Para et al., 2000) and either $AgNO_3$ or $HAuCl_4$ (Aldrich, 99.99%). Water solutions of $AgNO_3$ (1.5%, w/w) and $HAuCl_4$ (6%, w/w) were prepared.

DAS powder (Fiedorowicz & Para, 2006; Para et al., 2000) (2 g) was added to a deionized then distilled water (38 mL) and maintained at 80 °C on constant stirring. To aqueous suspensions of DAS, aliquots (1 mL) of either $AgNO_3$ or $HAuCl_4$ solutions (both from Aldrich, 99.99% purity) solutions were added, then aq. NH_3 solution (10%, w/w) (1 mL) was admixed. The reaction mixture was stirred for 10 min at 80 °C followed by cooling to room temperature. Resulting suspension of nanoAg or nanoAu in DAS matrix was centrifuged (5000 rpm) and dried at 50 °C to constant weight.

2.2. UV–vis absorption spectrophotometry

The UV–vis absorption spectra of DAS, DAS/nanoAg and DAS/nanoAu composites were recorded using a Shimadzu 2101 scanning spectrophotometer in the range of 200–700 nm using 10 mL cells. Concentration of solution was 0.001 g/cm^3.

2.3. FTIR-ATR spectrophotometry

The FTIR-ATR spectrum of the composites was recorded in the range of 4000–500 cm^{-1} at resolution of 4 cm^{-1} using a MATTSON 3000 FT-IR (Madison, Wisconsin, USA) spectrophotometer. That instrument was equipped with a 30SPEC 30 Degree Reflectance adapter fitted with the MIRacle ATR accessory from PIKE Technologies Inc., Madison, WI, USA.

2.4. Scanning and transmission electron microscopy (SEM and TEM)

Analyses of sizes and morphologies of the as-prepared nanoparticles were studied using a high resolution JEOL 7550 scanning electron microscope equipped with EDS analyzer for local chemical analysis. Because the material was sufficiently conducting, the gold sputter coating was dispensable.

2.5. High performance size exclusion chromatography (HPSEC-MALLS-RI)

DAS and nanocomposite samples (100 mg) moistened with water (10 mL) were suspended in dimethylsulfoxide (DMSO, 90 mL) then boiled for 12 h on agitation. Resulting solutions were filtered by 0.8 μm cellulose acetate filters (Whatman, England).

The high performance size exclusion chromatography (HPSEC) system for determination of average molecular weight and radii of gyration consisted of a pump (Shimadzu 10AC, Tokyo, Japan), an injection valve (model 7021, Rheodyne, Palo Alto, CA, USA), a guard column TSK PWH (Tosoh Corporation, Tokyo, Japan), and two connected size exclusion columns TSKgel GMPWXL (300 mm × 7.8 mm, Tosoh Corporation, Tokyo, Japan) and TSKgel 2500 PWXL (300 mm × 7.8 mm, Tosoh Corporation, Tokyo, Japan). A multiangle laser light scattering detector (MALLS) operating in chromatographic mode using a He–Ne laser light source (630.0 nm) (Dawn-DSP-F, Wyatt Technology, Santa Barbara, CA, USA) and a differential refractive index detector (L-7490, Merck, Darmstadt, Germany) were connected to the columns. The columns were maintained at 30 °C. The mobile phase (0.15 M $NaNO_3$ with 0.02% sodium azide) was filtered through 0.2 and 0.1 μm cellulose acetate filters (Whatman, England). The flow rate of the mobile phase and the sample injection volume were 0.4 mL/min and 500 μL respectively. The output voltage of refractive index (RI) and light scattering (LS) at 18 angles was used for calculation of the weight-average molecular weight (M_w) and radius of gyration (R_g) using Astra 4.73.04 software (Wyatt Technology, Santa Barbara, CA, USA).

2.6. Differential scanning calorimetry

For ~5 mg solid samples, the thermogravimetric analyses (TG) coupled with mass spectrometer (MS-TG/DTG/SDTA) were performed in Mettler-Toledo 851e apparatus in 150 μL corundum crucibles, closed by a lid with a hole, under flow of argon (80 mL/min), within temperature range 30–800 °C with heating rate of 10 °C/min. The simultaneous evolved gas analysis (EGA) was performed during the experiments by joined on-line quadruple mass spectrometer (QMS) (Thermostar Balzers).

The differential scanning calorimetry (DSC) experiments for the ~10 mg samples were performed in Mettler-Toledo 821e calorimeter equipped with an intracooler Haake in 40 μL aluminum crucibles under constant flow of argon (80 mL/min) within temperature range 25–400 °C.

2.7. X-ray diffractometry

X-ray powder diffractometry was performed according to Gérard, Colonna, Buléon, & Planchot (2001). Thus, samples of DAS and composites were adjusted to 200 g/kg of the water content. Equilibrated samples were sealed between two tape foils to maintain a stable water content throughout the measurement. Diffraction diagrams were recorded using X'pert type Phillips diffractometer with a cobalt lamp of $\lambda = 1.78896$ Å (30 mA and 40 kV) and in the scanning region of 2θ from 5 to 60° in 0.02° intervals.

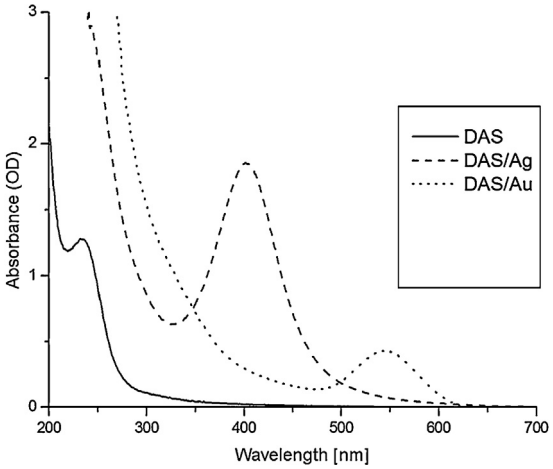

Fig. 1. UV–vis spectra of dialdehyde starch (DAS), DAS/nanoAg and DAS/nanoAu composites.

3. Results and discussion

Dialdehyde starch (DAS) served as both reducing and stabilizing agent during formation of nanoAg and nanoAu composites. After addition of $AgNO_3$ and $HAuCl_4$ to alkaline DAS suspensions reaction mixture turned yellow and dark red color, respectively, suggesting formation of the silver and gold nanoparticles. The UV–vis absorption spectra recorded for DAS and DAS/nanoAg and DAS/nanoAu composites are shown in Fig. 1. Spectra taken for nanoAg and nanoAu composites show the characteristic absorption maximum of Ag and Au nanoparticles centered at about 400 nm and 540 nm, respectively.

The sizes and morphologies of the as-prepared nanoparticles were studied with SEM/TEM microscopy. Typical SEM and TEM images of as-prepared nanoAg and nanoAu composites are shown in Figs. 2 and 3, respectively. In the case of nanoAg composites an evident formation of approximately spherical silver nanoparticles of the size within the range of 10–15 nm, inside the nanoscopic polysaccharide templates could be observed. SEM image (Fig. 2A) reveals morphology of DAS/nanoAg composite. It is clearly seen that polysaccharide chains form spherical crystals with sizes well under 100 nm. In the case of the nanoAu composites formation of the nanoparticles with almost uniform size of 8–10 nm, well dispersed in DAS matrix was observed.

The XRD pattern of the DAS and as-prepared DAS/nanoAg and DAS/nanoAu composites are shown in Fig. 4. The diffractograms present diffraction peaks at 2θ values of about 38.4, 44.5, 64.7 for nanoAu composites and 38.1, 44.4 and 64.7 for nanoAg composites. They are relevant to the metal nanocrystals. Measured positions of the diffraction peaks of the as-prepared nanoAu and nanoAg particles in the DAS matrix correlate well with previously reported results (Chairam, Channarong, & Ekasith, 2009). The formation of the nanoparticle containing DASs had an absolutely minor influence on the crystallinity of the preparations as deduced from the pattern of the major intensive, broad peak centered at 19 2θ. The highly intensive peaks observed in the diffractograms of samples are (1 1 1) reflection. The (2 0 0) and (2 2 0) peaks are less intense. So, in this case, we might conclude that the nano-assemblies were mainly composed of (1 1 1) lattice planes. The diffraction peaks are broad pointing to very small size of the crystallites (Irshad, Aparna, Jahangeer, & Tokeer, 2011). The XRD shows that silver and gold

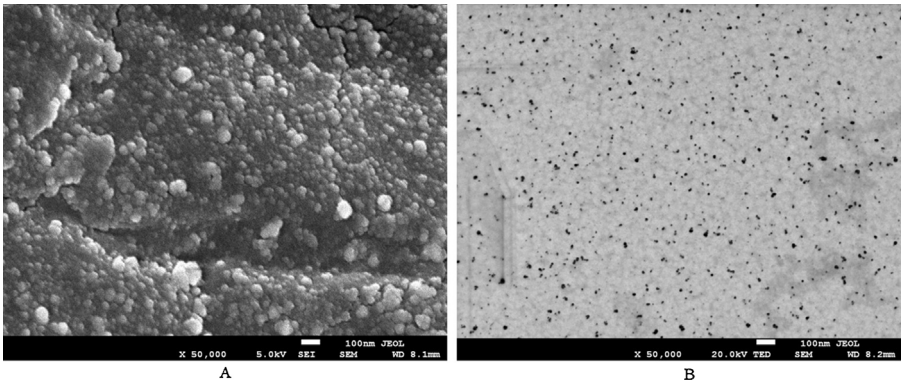

Fig. 2. SEM (A) and TEM (B) images of DAS/nanoAg composites.

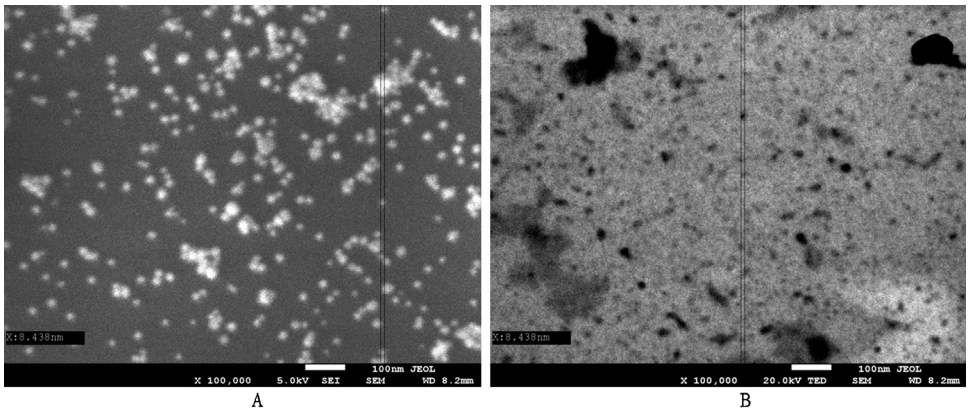

Fig. 3. SEM (A) and TEM (B) images of DAS/nanoAu composites.

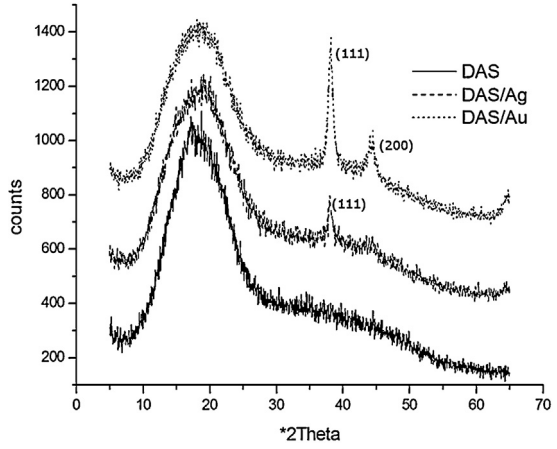

Fig. 4. The XRD pattern of DAS and as-prepared DAS/nanoAg and DAS/nanoAu composites.

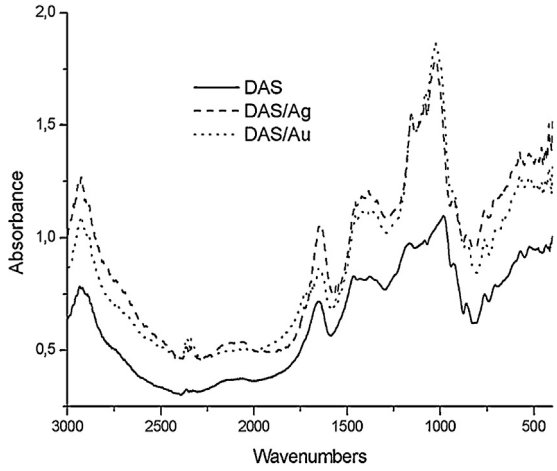

Fig. 5. The FTIR spectra of DAS, DAS/nanoAg and DAS/nanoAu composites.

nanoparticles formed are crystalline. Based on the Debye-Scherrer formula (Cullity, 1978) the average size of the Ag and Au nanoparticles is 11.3 and 9.6 nm, respectively.

FTIR spectra of DAS as well as DAS/nanoAg and DAS/nanoAu composites are shown in Fig. 5. In the spectrum of original DAS the aldehyde carbonyl group could be seen as longer wavelength shoulder of the more intensive band of vibrations from water arrested in the DAS matrix (Raveendran et al., 2003). In the spectra of DAS/nanoAg and DAS/nanoAu the latter band increased its intensity likely to the participation of the asymmetric vibrations of the COO^-. Also essential change in the pattern of the complex band in the area specific for the symmetric vibrations of in the COO^- group can provide an evidence of the reducing role of DAS in generation of metal nanoparticles in the performed synthesis.

Table 1
Absolute molecular weight M_w and radii of gyration R_g of the polysaccharide chains from dialdehyde starch (DAS), DAS/nanoAg and DAS/nanoAu composites.

Sample	$M_w \times 10^5$	R_g (nm)
DAS	0.18	85.1
DAS/nanoAg	2.29	57.7
DAS/nanoAu	2.20	86.1

The thermal properties of DAS as measured by DSC, differ significantly from the thermal properties of DAS/nanoAg and DAS/nanoAu (Fig. 6A). Patterns of the DAS thermogram indicate occurrence of glass – rubber transition (T_g = 221 °C) followed by exothermic peak centered at 296 °C which could be attributed to decomposition of DAS. Thermograms recorded for DAS/nanoAg and DAS/nanoAu exhibit two exothermic peaks. The first of them centered at 249 °C common for both DAS/nanoAg and DAS/nanoAu thermograms could be associated with crystallization of the matrix polysaccharide chains. The second peak with maximum at 298 °C for DAS/nanoAg and 302 °C for DAS/nanoAu could be associated with the composite degradation. For both composites, thermograms patterns indicate that glass rubber – transition did not occur. Differences in thermal properties between DAS, DAS/nanoAg and DAS/nanoAu could be explained by rearrangements mainly polymerization, of DAS polysaccharide chains during reduction of $AgNO_3$ and $HAuCl_4$ by DAS molecules.

Both, DAS/nanoAg and DAS/nanoAu contained by approximately 1% water less than original DAS as shown in Fig. 6B presenting TGA curves of those preparations. Also, the slope of the decomposition the nanoparticle containing DAS suggested their slightly faster decomposition than that of DAS itself.

Results of the molecular weight estimations for these species fit such assumption (Table 1). Weight average molecular weight M_w of DAS molecules was very low (0.18×10^5) as compared to native starch, due to severe degradation of starch molecules during oxidation reaction. However, significant rise of M_w up to 2.2×10^5 was observed for molecules constituting DAS/nanoAg and DAS/nanoAu. It is evident that on the reduction of the Ag and Au ions by DAS, polymerization and/or crosslinking of DAS chains occurred. Data collected from detectors in course of the size exclusion chromatographic estimations provided calculations of the differential molar mass distribution. The differential molar mass distribution gave the amount of material (differential weight fraction) in a given molar mass interval, a good indicator of the polydispersity of the

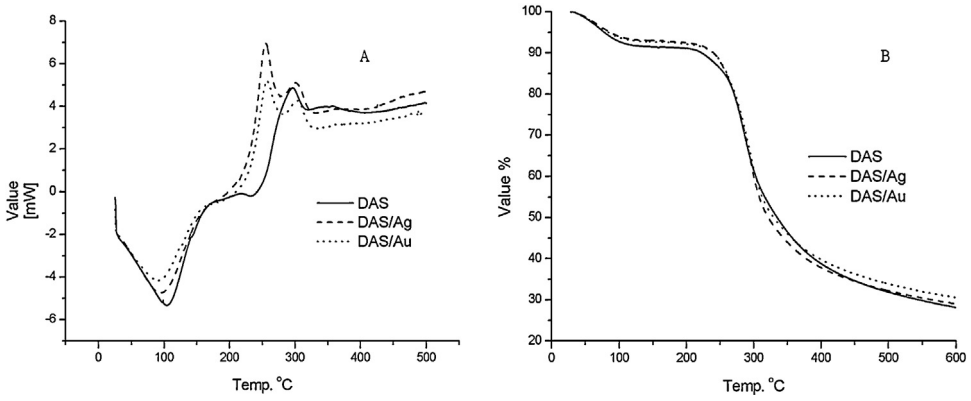

Fig. 6. DSC thermograms (A) and TGA curves (B) of DAS (solid line), DAS/nanoAg (dotted line) and DAS/nanoAu (pointed line) composites.

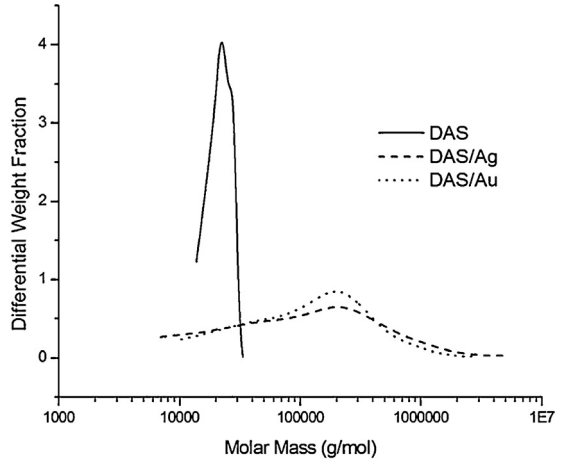

Fig. 7. Plots of differential molar weight distribution in DAS, DAS/nanoAg and DAS/nanoAu polysaccharide chains (solid, dotted and pointed lines, respectively).

polymer. The plots of the differential molar mass distribution for DAS, DAS/nanoAg and DAS/nanoAu are given in Fig. 7. Clearly, DAS molecules exhibited a low polydispersity and their molecular weight did not exceed 3×10^5 whereas molecular weight of the chains in DAS/nanoAg and DAS/nanoAu ranged from 1×10^4 to 7×10^6.

4. Conclusion

Silver and gold nanoparticles have been successfully prepared by environmentally friendly method, using dialdehyde starch acting as stabilizing template and reducing agent.

Polymerization and/or crosslinking of polysaccharide chains observed during formation of nano Ag and nano Au structures in the presence of DAS molecules led to significant changes in thermal and structural properties of polysaccharide matrix resulting in nanosilver and nanogold composites of unique properties.

Acknowledgements

This work was financed by grant: N R12 0015 06 from The Polish National Centre for Research and Development (NCBiR).

References

Adhyapak, P. V., Singh, N., Vijayan, A., Aiyer, R. C., & Khanna, P. K. (2007). Single mode wave guide properties of m-NA doped Au/PVA nano-composites: Synthesis, characterization and studies. *Materials Letters*, *61*, 3456–3461.

Bradley, J. S. (1994). In G. Schmid (Ed.), *Clusters and colloids* (pp. 459–544). Weinheim: Wiley-VCH.

Brown, D. H., & Smith, W. E. (1980). Chemistry of gold drugs in the treatment of rheumatoid arthritis. *Chemical Society Reviews*, *9*, 217–240.

Brust, M., Walker, M., Bethell, D., Schiffrin, D. J., & Whyman, R. (1994). Synthesis of thiol-derivatized gold nanoparticles in a two-phase liquid–liquid system. *Journal of the Chemical Society. Chemical Communications*, 801–802.

Chairam, S., Channarong, P., & Ekasith, S. (2009). Starch vermicelli template-assisted synthesis of size/shape-controlled nanoparticles. *Carbohydrate Polymers*, *75*, 694–704.

Cullity, B. D. (1978). *Elements of X-ray diffraction* (2nd ed.). Reading, MA: Addison-Wesley.

Dabbagh, M. A., Moghimipour, E., Ameri, A., & Sayfoddin, N. (2008). Physicochemical characterization and antimicrobial activity of nanosilver containing hydrogels. *Iranian Journal of Pharmaceutical Research*, *7*(1), 21–28.

Daniel, M. C., & Astruc, D. (2004). Gold nanoparticles: Assembly, supramolecular chemistry, quantum-size-related properties, and applications toward biology, catalysis, and nanotechnology. *Chemical Reviews*, *104*, 293–346.

Datta, K. K. R., Srinivasan, B., Balaram, H., & Eswaramoorthy, M. (2008). Synthesis of agarose-metal/semiconductor nanoparticles having superior bacteriocidal activity and their simple conversion to metal–carbon composites. *Journal of Chemical Sciences*, *120*, 579–586.

Fiedorowicz, M., & Para, A. (2006). Structural and molecular properties of dialdehyde starch. *Carbohydrate Polymers*, *63*, 360–366.

Fu, Y., Yang, Y., Li, J., Yu, K. D., & Long, J. (2006). Formation of cotton-like nanogold assembly and their fluorescence property. *Nanotechnology*, *17*, 5147–5150.

Frens, G. (1973). Controlled nucleation for the regulation of the particle size in monodisperse gold suspensions. *Nature (London), Physical Sciences*, *241*, 20–22.

Gérard, C., Colonna, P., Buléon, A., & Planchot, V. (2001). Amylolysis of maize mutant starches. *Journal of the Science of Food and Agriculture*, *81*, 1281–1287.

Giersig, M., & Mulvaney, P. (1993). Preparation of ordered colloid monolayers by electrophoretic deposition. *Langmuir*, *9*, 3408–3413.

Hayat, M. A. (1989). *Colloidal gold, principles, methods and applications*. New York: Academic Press.

Hiramatsu, H., & Osterloh, F. E. (2004). A simple large-scale synthesis of nearly monodisperse gold and silver nanoparticles with adjustable sizes and with exchangeable surfactants. *Chemistry of Materials*, *16*, 2509–2511.

Huang, L., Guo, Z. R., Weng, M., & Gu, N. (2006). Facile synthesis of gold nanoplates by citrate reduction of $AuCl_4^-$ at room temperature. *Chinese Chemical Letters*, *17*, 1405–1408.

Huang, H., & Yang, X. (2004). Synthesis of polysaccharide-stabilized gold and silver nanoparticles: A green method. *Carbohydrate Research*, *339*, 2627–2631.

Hyatt, A. D., & Eaton, B. T. (1993). *Immuno-gold electron microscopy in virus diagnosis and research*. Boca Raton, FL: CRC Press.

Irshad, A. W., Aparna, G., Jahangeer, A., & Tokeer, A. (2011). Silver nanoparticles: Ultrasonic wave assisted synthesis, optical characterization and surface area studies. *Materials Letters*, *65*, 520.

Kang, B., & Wu, J. W. (2006). Fabrication of gold/polyvinyl-alcohol nano-composites by photoreduction and their optical characterization. *Journal of the Korean Physical Society*, *49*, 955–958.

Kim, J. (2007). Antibacterial activity of Ag+ ion-containing silver nanoparticles prepared using the alcohol reduction method. *Journal of Industrial and Engineering Chemistry*, *13*, 718–722.

Kumar, S., Abhilash, S., Manzoor, K., Nair, S. V., Tamura, H., & Jayakumar, R. (2010). Preparation and characterization of novel β-chitin/nanosilver composite scaffolds for wound dressing applications. *Carbohydrate Polymers*, *80*, 761–767.

Leff, D. V., Brandt, L., & Heath, J. R. (1996). Synthesis and characterization of hydrophobic, organically-soluble gold nanocrystals functionalized with primary amines. *Langmuir*, *12*, 4723–4730.

Li, X., Hao, X., & Hui, N. (2007). Preparation of nanosilver particles into sulfonated poly(ether ether ketone) (S-PEEK) nanostructures by electrospinning. *Materials Letters*, *61*, 421–426.

Lin, J. P., Tseng, Y. C., & Chien, H. S. (2006). Method for manufacturing antibacterial polyester master batches and fibers both containing nanosilver particles. US Patent 7052765.

Merchant, B. (1998). Gold, the noble metal and the paradoxes of its toxicology. *Biologicals*, *26*, 49–59.

Pal, A., Shah, S., & Devi, S. (2007). Synthesis of Au, Ag and Au–Ag alloy nanoparticles in aqueous polymer solution. *Colloids and Surface A: Physicochemical and Engineering Aspects*, *302*, 51–57.

Pal, S., Tak, Y. K., & Song, J. M. (2007). Does the antibacterial activity of silver nanoparticles depend on the shape of the nanoparticle? A study of the gram-negative bacterium *Escherichia coli*. *Applied and Environmental Microbiology*, *73*, 1712–1720.

Para, A., Karolczyk-Kostuch, S., Hajdon, T., & Tomasik, P. (2000). Dialdehyde starch of low degree of oxidation and its derivatives. *Polish Journal of Food and Nutrition Sciences*, *9*(2), 7–12.

Park, J., Lee, D. J., Kim, S. J., & Oh, J. H. (2009). Dynamic characteristics measurements of inkjet-printed thin films of nanosilver suspensions on a flexible plastic substrate. *Journal of Micromechanics and Microengineering*, *19*, 095021.

Pobedinsky, M., & Johnston, J. (2010). Nanogold and nanosilver plastics. In *Proceedings of the TechConnect NSTI Nano Science and Technology Institute Conference* Anaheim,. http://www.techconnectworld.com/World2010/a.html?i=318

Raveendran, P., Fu, J., & Wallen, S. L. (2003). Completely "green" synthesis and stabilization of metal nanoparticles. *Journal of the American Chemical Society*, *125*, 13940–13941.

Saulon, C., Despax, B., Mercier-Bonin, M., Marcus, P., Zanna, S., & Raynaud, P. (2008). Plasma-engineered polymer thin films with embedded nanosilver for prevention of microbial adhesion. In *E-MRS fall meeting Warsaw, Poland, 2008, on-line journal of symposium* September 18th.

Schmid, G. (1992). Review large clusters and colloids. Metals in the embryonic state. *Chemical Reviews*, *92*, 1709–1727.

Shon, Y.-S., & Choo, H. (2003). Dendrimers, nanosciences, & D. Astruc (Eds.), *Organic reactions of monolayer-protected metal nanoparticles* (6) (pp. 1009–1018). Paris: C. R. Chime.

Song, L., Cruz, C., Farrah, S. R., & Baney, R. H. (2009). Novel antiviral activity of dialdehyde starch. *Electronic Journal of Biotechnology*, *12*, 1–5.

Templeton, A. C., Wuelfing, W. P., & Murray, R. W. (2000). Monolayer-protected cluster molecules. *Accounts of Chemical Research*, *33*, 27–36.

Tokuda, S., Obata, A., & Kasuga, T. (2009). Preparation of poly(lactic acid)/siloxane/calcium carbonate composite membranes with antibacterial activity. *Acta Biomaterialia*, *5*, 1163–1168.

Turkevitch, J., Stevenson, P. C., & Hillier, J. (1951). A study of the nucleation and growth processes in the synthesis of colloidal gold. *Discussions of the Faraday Society*, *11*, 55–57.

Tzhayik, O., Sawant, P., Efrima, S., Kovalev, E., & Klug, J. T. (2002). Xanthate capping of silver, copper, and gold colloids. *Langmuir*, *18*, 3364–3369.

Wu, S. H., & Chen, D. H. (2004). Synthesis of high-concentration Cu nanoparticles in aqueous CTAB solutions. *Journal of Colloid and Interface Science*, *273*, 165–169.

Vasilev, A. N., Gulliver, E. A., Khinast, J. G., & Riman, R. E. (2009). Highly dispersible polymer-coated silver nanoparticles. *Surface and Coatings Technology*, *203*, 2841–2844.

Xu, M., Feng, J. Q., & Cao, X. I. (2008). Electrical properties of nano-silver/polyacrylamide/ethylene vinyl acetate composite. *Journal of the Shanghai University (English Edition)*, *12*, 85–90.

Yonezawa, T., & Kunitake, T. (1999). Practical preparation of anionic mercapto ligand-stabilized gold nanoparticles and their immobilization. *Colloids and Surfaces A: Physicochemical and Engineering Aspect*, *149*, 193–199.

Zhang, K., Fu, Q., Fan, J., & Zhou, D. (2005). Preparation of Ag/PS composite particles by dispersion polymerization under ultrasonic irradiation. *Materials Letters*, *59*, 3682–3686.

Zhua, H. T., Zhang, C. Y., & Yin, Y. Y. (2004). Rapid synthesis of copper nanoparticles by sodium hypophosphite reduction in ethylene glycol under microwave irradiation. *Journal of Crystal Growth*, *270*, 722–728.